FTIR and Raman spectra of CH(D)FCl–CF2–O–CHF derivatives of enflurane. Experimental and ab initio study

ARTICLE *in* CHEMICAL PHYSICS · APRIL 2015

Impact Factor: 1.65 · DOI: 10.1016/j.chemphys.2015.03.010

6 AUTHORS, INCLUDING:

Sona M Melikova
Saint Petersburg State University
64 PUBLICATIONS **524** CITATIONS

SEE PROFILE

W. A. Herrebout
University of Antwerp
185 PUBLICATIONS **3,352** CITATIONS

SEE PROFILE

Chemical Physics 453-454 (2015) 26–34

Contents lists available at ScienceDirect

Chemical Physics

journal homepage: www.elsevier.com/locate/chemphys

FTIR and Raman spectra of CH(D)FCl—CF_2—O—CHF derivatives of enflurane. Experimental and ab initio study

S.M. Melikova [a], K.S. Rutkowski [a,*], E. Telkova [a,c], B. Czarnik-Matusewicz [b], M. Rospenk [b], W. Herrebout [c]

[a] Department of Physics, Saint-Petersburg State University, Ulianovskaja 3, 198504 St.Petersburg, Russia
[b] Faculty of Chemistry, University of Wroclaw, Joliot Curie 14, 50-383 Wroclaw, Poland
[c] Department of Chemistry, University of Antwerp, Groenenborgelaan 171, B-2020 Antwerp, Belgium

ARTICLE INFO

Article history:
Received 28 January 2015
In final form 30 March 2015
Available online 4 April 2015

Keywords:
Enflurane
IR and Raman spectra
Anharmonicity
Ab initio calculations
Conformation
H bond

ABSTRACT

The vibrational spectra of two H/D derivatives of enflurane are studied with the help of FTIR cryospectroscopy in liquefied Kr and Raman spectroscopy of pure liquid. The majority of fundamental bands are identified. Using MP2/6-311++G(df,pd) calculations the six local minima are found on the potential energy surface and ascribed to the most stable conformers of enflurane. The vibrational frequencies, infrared intensities, and Raman activities are found at the same level of theory. The potential energy distribution is calculated for the most stable conformer. Assignment of the vibrational bands registered is performed using the results of calculations of the frequencies with "anharm" option implemented in Gaussian. The model IR and Raman spectra built with the help of data of ab initio calculations reflect the basic features of experimental spectra. IR spectra of cryosolutions of enflurane and acetone in liquefied Kr suggest weak complex formation stabilized by "blue shifting" H bonds.

1. Introduction

The importance of weak intermolecular interactions involving so called CH donors in chemical and biochemical applications is commonly recognized. The widest class of such donors belongs to multiply halogenated alkanes. Some of them, e.g. CHF_3 and $CHCl_3$ can form H – bonds with unusual spectroscopic and geometric features [1–11]. Modern volatile anesthetics possess at least one CH group which might participate in weak noncovalent intermolecular interactions. Recent experimental and theoretical studies have clearly shown that such general anesthetic as halothane ($CHClBrCF_3$) participates in complex formation stabilized by weak H – bond of CH...B (B = O, N, F) or CH...π type [12–14].

The consideration of preferable possible paths of intermolecular H – bond formation becomes more complicated in the case of such anesthetics as halogenated derivatives of ethers having two CH groups. Enflurane ($CHFCl—CF_2—O—CHF_2$) is typical example. As other compounds having asymmetric carbon atoms, it is synthesized and used as a racemic mixture of the *R* and *S* enantiomers. As a result, such a natural mixture is optically inactive and only conventional IR and Raman spectra might be studied. The spatial geometry of enflurane, specifically various orientation of three single bonds in the C—C—O—C skeleton, suggest possible existence at least of different 27 conformational forms. This might result in rich vibrational spectrum of enflurane, with numerous bands assigned to the same normal vibration. In the earlier study based on ab initio MP2/6-311G(2d) calculations, the most stable four conformers were postulated [15]. Qualitatively analogous conclusion was made by the help of comparison of experimental IR spectra of enflurane dissolved in CCl_4 with results of DFT calculations on B3LYP/6–31G(d) level [16]. Meanwhile results of gas electron diffraction were reproduced best considering a mixture of three conformers [15].

Due to nonequivalent electron withdrawing properties of neighbor F and Cl atoms the two CH groups located at opposite parts of enflurane can act as proton donors of different energetic and spectroscopic properties. Recent results on theoretical studies and room temperature spectroscopic measurements performed for enflurane + acetone system confirm the mentioned feature of CH groups [17]. The blue shift and different change of the intensity of CH stretching vibration localized on the CHFCl and CHF_2 groups have been interpreted considering the geometric features of the dipole moment function [18,19]. However the bands registered at room temperature in pure liquid enflurane or in concentrated solution in conventional CCl_4 solvent are noticeably broadened or sometimes unresolved at all. Additionally interpretation of the IR spectra can be complicated due self association of nearly placed molecules.

* Corresponding author.
E-mail address: rutkowsk@molsp.phys.spbu.ru (K.S. Rutkowski).

http://dx.doi.org/10.1016/j.chemphys.2015.03.010
0301-0104/

The present study revisits a comprehensive consideration of enflurane both by the method of cryospectroscopy and by a set of ab initio MP2 calculations utilizing the Pople-type 6-311++G(df,pd) basis set. The IR spectra of enflurane dissolved in liquefied Kr ($T \sim 120$–155 K) have been registered. The frequency range amounts c.a. 800–7500 cm^{-1}. Additionally to the IR cryosolution measurements, Raman spectra of liquid enflurane have been measured at room temperature in the range c.a. 150–3500 cm^{-1}. To get better interpretation in particular parts of vibrational spectra of enflurane, the derivative of enflurane with H/D exchange at the chlorofluoromethyl carbon was also synthesized and used. The deepest 6 real minima, having close values of energy, were found on the potential energy surface (PES).

The experimental spectra have been compared with the theoretical spectra to assign the bands registered. Relative contributions from the most stable conformers of enflurane were taken into account in this simulation.

2. Experimental and computational methods

The IR spectra of enflurane were registered using Nicolet Nexus and Nicolet – 6700 FTIR spectrometers, in the range ~800–7500 cm^{-1} with a resolution of 0.2–0.5 cm^{-1}. The number of scans was varied between 100 and 300. Liquefied Kr was used as an inert solvent in which the solubility of enflurane was relatively good. Measurements have been performed at $T \sim 120$–155 K. A home-made cryostat was equipped by a stainless-steel cell of 5 cm optical length. BaF_2 windows were sealed by indium gaskets. The temperature was monitored both by Cu/Constantan thermocouple attached to the body of the cell, and by measuring the vapor pressure over the liquid solutions. The accuracy of temperature measuring was believed better than 3 K. The concentration of enflurane was kept in the range of ~10^{17}–10^{18} molecules/cm^3.

Raman spectra of pure liquid enflurane were recorded in 50–3500 cm^{-1} spectral range with a resolution of 2.5 cm^{-1} using FT Raman Bruker Multiram unit equipped by LN_2 – cooled germanium detector. The number of scans amounts 1024. The excitation of the sample was performed by CW Nd:YAG laser at 200 mW and frequency ~9394 cm^{-1}. The 180° backscattering geometry/collection optics has been used for collection the scattered radiation. The spectra were measured at room temperature.

The H/D exchange at the chlorofluoromethyl carbon of enflurane has been performed according the reaction described in Ref. [20]. Shortly, heating the mixture of enflurane and ~0.4 M of NaOD to reflux for ~20–24 h resulted in c.a. 70–85% exchange at the chlorofluoromethyl carbon. This result is quite satisfactory for spectroscopic measuring and assignments of selected bands.

Theoretical calculations were performed using the GAUSSIAN 09 Rev. C.01 [21]. The local minima were searched by relaxed potential energy surface (PES) scan calculations with geometry optimization at each point. The step of 2° has been chosen for these scans. In accordance with the spatial geometry of enflurane (HFClC—CFF—O—CFFH), the scans over each of three dihedral angles were selected on the final stage of local minima searching. One angle was defined by four atoms of skeleton (C—C—O—C). Other two were built substituting one of the end (terminal) C atoms by Cl or H atom. All the local minima found were fully optimized using ab initio second order Møller-Plesset perturbation (MP2) frozen core method [22] with the Pople-type 6-311++G(df,pd) basis set. The basis set has been chosen as a compromise between the accuracy of calculations and the available computing resources. The conformations were characterized as these local minima having all real (positive) frequencies. The harmonic frequencies were calculated first. Relative contribution of separate internal coordinates to the normal modes of enflurane has been evaluated using results of potential energy distribution (PED) calculations. PED was calculated according to Ref. [23]. The PED values were close to those obtained with the help of the conventional GAR2PED program. They were also controlled by visual inspection for each vibrations using Gaussian view. The procedure of the normal coordinate analysis was analogous to that described in Ref. [24]. To improve the comparison procedure between experimental and calculated spectra of enflurane, the final spectroscopic parameters have been calculated using the option "anharm".

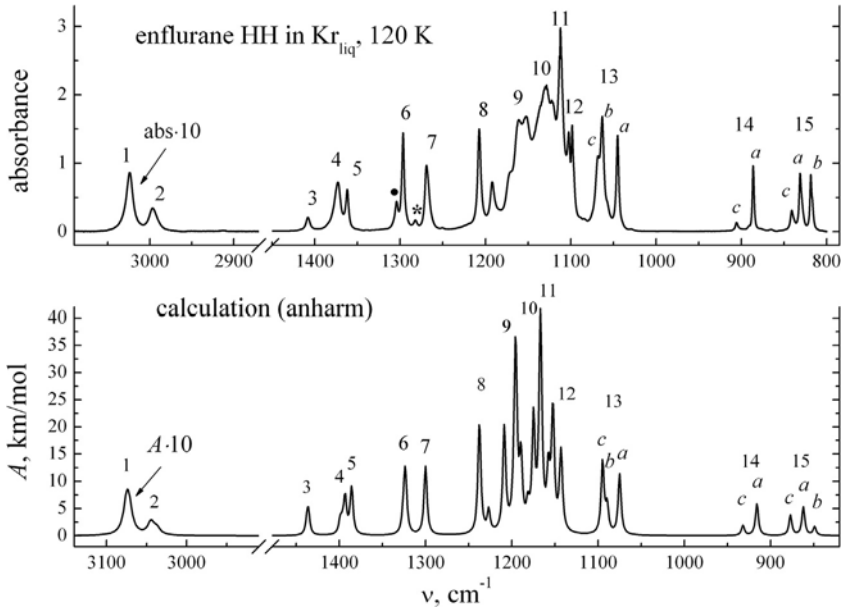

Fig. 1. The IR spectrum of enflurane HH (CHFCl—CF_2—O—CHF_2). Top panel – experimental spectrum in liquid Kr at $T \sim 120$ K, n(CHFCl—CF_2—O—CHF_2) ~ $2 \cdot 10^{17}$ molecules/cm^3; tentative assignment: • – $\nu_{15} + \nu_{21} \sim \nu_6$, * – $\nu_{15} + \nu_{22} \sim \nu_7$. Bottom panel – calculated spectrum. Weak CH bands are scaled by a factor of 10 for convenience. *a*, *b*, *c* – the bands ascribed to conformers *a*, *b*, *c*.

3. Results of measurements

Fig. 1 (top panel) displays the IR spectrum of diluted solution of enflurane HH (CHFCl—CF_2—O—CHF_2) in liquid Kr in the region ~800–3200 cm^{-1}. The two weak bands near 3000 cm^{-1} are scaled by a factor of 10 for convenience. They correspond to CH stretching vibrations ν_1 and ν_2. Wholly overlapped bands situated near ~1100–1200 cm^{-1} correspond to CF stretching vibrations. They might be noticeably modified by the transition dipole – transition dipole interactions of nearly placed molecules in the case of higher concentrations or liquid enflurane [25]. The region of overtone bands was considered in the previous paper [19]. The IR spectrum of enflurane HD (CDFCl—CF_2—O—CHF_2) is shown on top panel of Fig. 2. The high frequency CH stretch ν_1 remains at the same position. Naturally, it relates to CH of CHF_2 group. The low frequency CH stretch ν_2 is expected to be appeared in the region of ~2200–2300 cm^{-1}. However it is hardly detected, because it is hidden between numerous combination bands of comparable strength. At last, it is worth noting the broadening temperature effect for all the bands registered.

Raman spectra of liquid enflurane HH and enflurane HD have been measured at room temperature. Because Raman scattering activity S_i (in $Å^4$/amu) is the result of ab initio calculations, the measured scattering cross section $\left(\frac{d\sigma}{d\Omega}\right)_\nu$ has been used to obtain the experimental scattering activity coefficient [26,27]:

$$S_{exp} \sim \left(\frac{d\sigma}{d\Omega}\right)_\nu \frac{\nu(1-\exp(-hc\nu/kT))}{(\nu_0-\nu)^4} \quad (1)$$

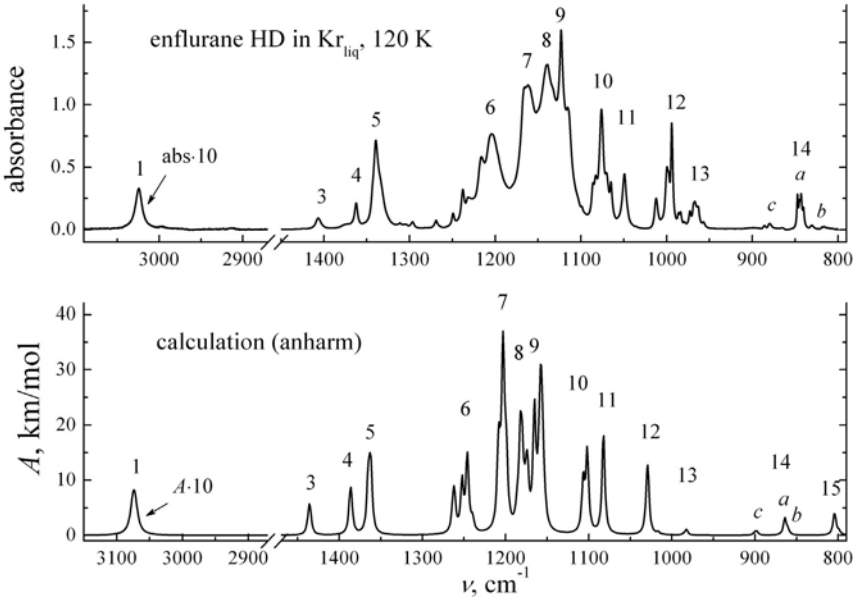

Fig. 2. The IR spectrum of enflurane HD (CDFCl—CF_2—O—CHF_2). Top panel – experimental spectrum in liquid Kr at $T \sim 120$ K, n(CDFCl—CF_2—O—CHF_2) ~ 10^{17} molecules/cm^3. Bottom panel – calculated spectrum. Weak CH bands are scaled by a factor of 10 for convenience. *a*, *b*, *c* – the bands ascribed to conformers *a*, *b*, *c*.

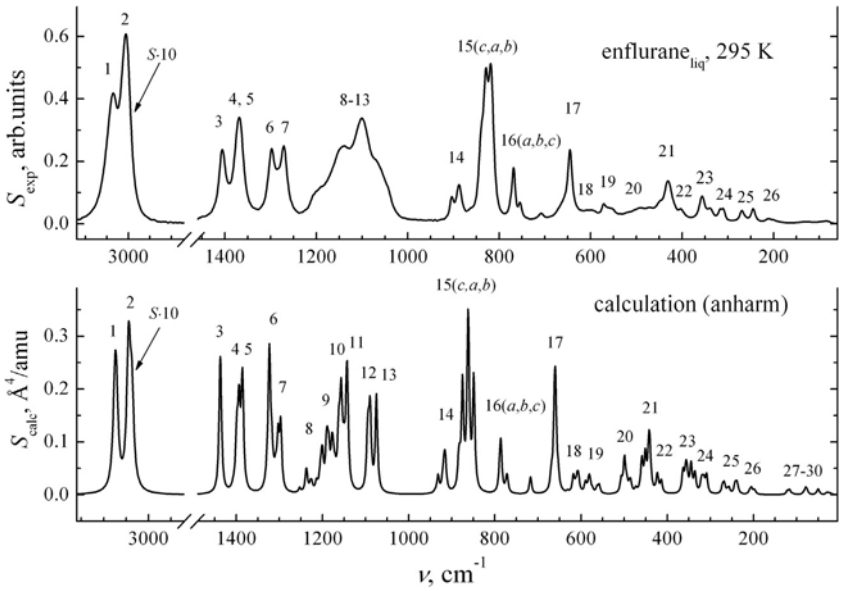

Fig. 3. The Raman spectrum of enflurane HH (CHFCl—CF_2—O—CHF_2). Top panel – experimental spectrum of liquid enflurane at $T \sim 295$ K. Bottom panel – calculated spectrum. CH bands are scaled by a factor of 10 for convenience.

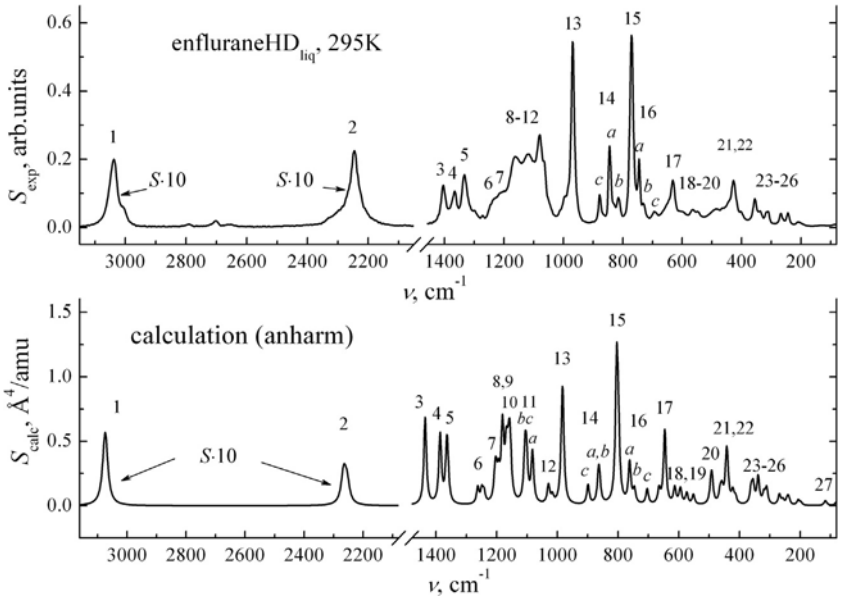

Fig. 4. The Raman spectrum of enflurane HD (CDFCl—CF_2—O—CHF_2). Top panel – experimental spectrum of liquid enflurane at $T \sim 295$ K. Bottom panel – calculated spectrum. CH and CD bands are scaled by a factor of 10 for convenience.

where ν_0 ~9394 cm^{-1} is the wavenumber of excitation laser. The results are presented on top panels of Figs. 3 and 4 respectively.

Despite the IR spectrum where the detection of band ν_2 is unsuccessful, this CD stretch localized on CDFCl group is registered at ~2247 cm^{-1} as a band of middle strength. Previous IR studies performed in pure liquid and in concentrated solutions in conventional CCl_4 solvent have shown that enflurane might form dimers and higher associates [16,17]. This conclusion was made analyzing the region of these CH stretch bands. In the case of Raman spectrum of liquid enflurane, it is reasonable to suppose that it consists of fundamental bands of monomeric species predominantly. The most valuable information, obtained from the Raman spectra refers to the vibrational bands of enflurane below ~ 800 cm^{-1}.

4. Results of calculations and discussion

Fig. 5 presents six conformers which correspond to the deepest (real) local minima found in the course of scan calculations over dihedral angles χ_1 (Cl_2—C_1—C_5—O_8) – Fig. 6, χ_2 (H_{10}—C_9—O_8—C_5) – Fig. 7, and χ_3 (C_1—C_5—O_8—C_9). The conformers are denoted as *a*, *b*, *c* going from largest to the smallest dihedral angle χ_1 (see Fig. 6). This corresponds to rotation of $C_1Cl_2F_3H_4$ group around the C_1—C_5 axis predominantly. Subscript 1 or 2 refers to a negative or positive value of χ_2 (see Fig. 7).It is rotation of $C_9H_{10}F_{11}F_{12}$ group around the C_9 – O_8 axis. Fig. 7 clearly shows that the barrier between 1 and 2 conformers is very small. Nevertheless all the 6 minima are characterized by real (positive) frequencies. Selected geometric parameters are collected in Table 1. The lowest minimum corresponds to conformer a_2. Conformer a_1 has a little bit higher energy. However, the thermodynamic analysis based on ab initio calculations shows the conformer a_1 is the most populated in the temperature range of our measurements. Conformer b_2 is situated higher than the conformer a_2 by about 113 cm^{-1}. The rests are placed between those.

The calculated spectroscopic parameters and the potential energy distribution (PED) of conformer a_1 are presented in Table 2 for enflurane HH and in Table 3 for enflurane HD. Additionally to harmonic also anharmonic frequencies are reported. In this work we restricted the anharmonic calculations to those, implemented in GAUSSIAN 09 Rev. C.01 program.

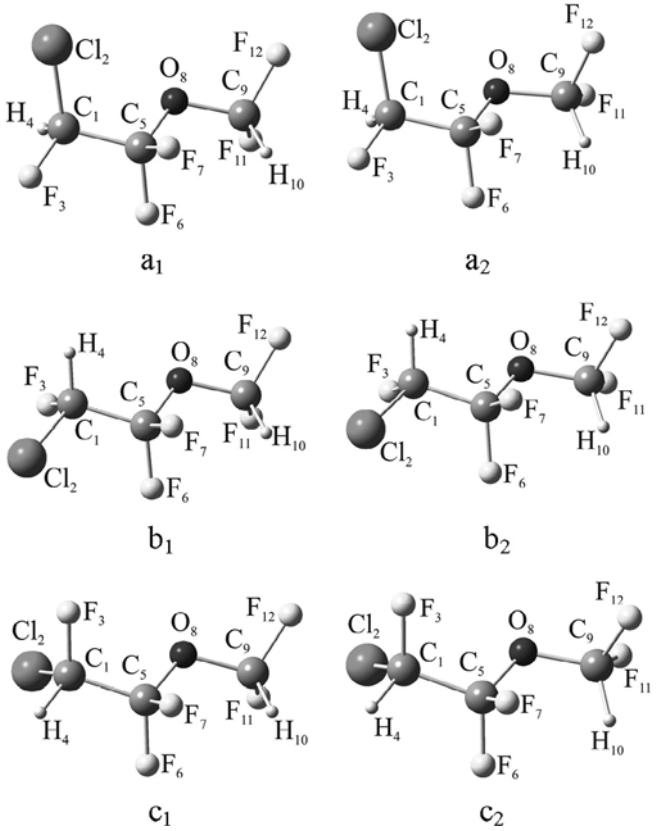

Fig. 5. MP2/6-311++G(df,pd) optimized structures of the most stable conformers of enflurane.

Considering a numerous set of Fermi resonances which are omitted in this program, could give additional correction for frequencies, intensities and Raman activities. Generally, results of the present PED analysis are compatible with those performed in earlier work [16]. The serious disagreement is found only in the case of ν_4 and ν_5 vibrations. Our data obtained at noticeably higher level of theory

are additionally confirmed by comparative analysis of PED for enflurane HH and enflurane HD. It should be noted, that vibrations ν_1, ν_2, ν_3, have the same PED for both isotopic forms of enflurane. Whereas PED is noticeably different in the case of modes with atom D engaged. At last the difference practically disappears for low frequency vibrations in which heavy atoms and atoms of skeleton are participated. The spectroscopic parameters calculated for all the six conformers are given in Supporting Information section (Table 1S).

The calculated spectra have been drawn taking into account relative populations P_i of the six conformers, found in ab initio MP2/6-311++G(df,pd) calculations:

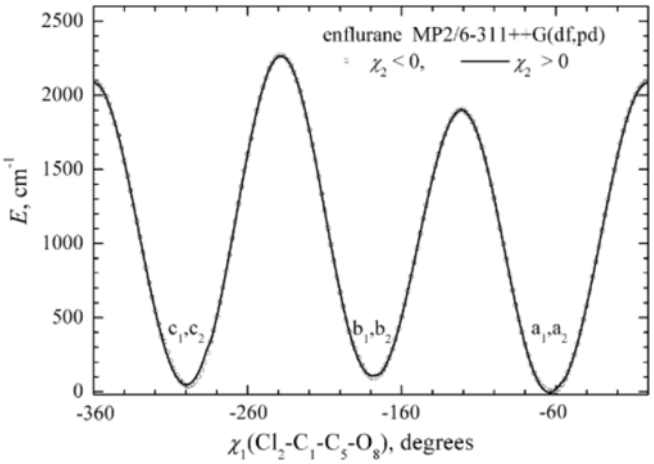

Fig. 6. The relaxed PES scan over the dihedral angle $\chi_1 = (Cl_2—C_1—C_5—O_8)$.

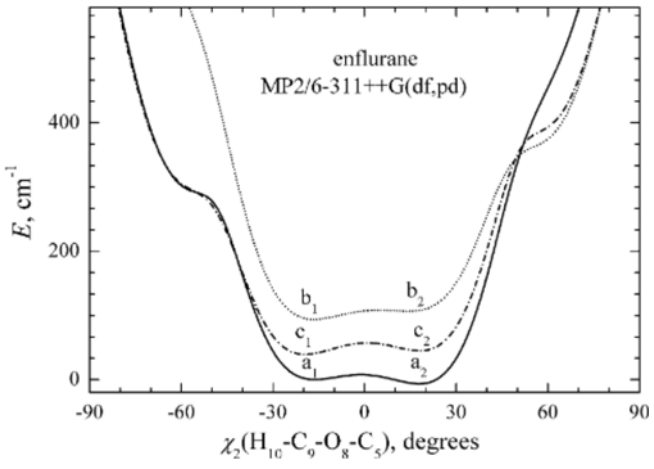

Fig. 7. The relaxed PES scan over the dihedral angle $\chi_2 = (H_{10}—C_9—O_8—C_5)$.

$$P_i = \frac{\exp(-\Delta G_i/kT)}{\sum_i \exp(-\Delta G_i/kT)} \quad (2)$$

where $\Delta G_i = G_i - G_0$ – the difference between the Gibbs Free Energy of ith conformer and the Gibbs Free Energy of the most stable conformer a_1. Results of these calculations are presented in Supporting Information section (Tables 2S and 3S). The profiles of the majority of bands of heavy tops registered in low temperature inert solvent are close to the Lorentz [28,29]. Thus, the bands of each conformer were modeled by the Lorentz profile:

$$L_j(\nu - \nu_{0j}) = \frac{\Gamma_j}{\pi} \cdot \frac{1}{(\nu - \nu_{0j})^2 + \Gamma_j^2} \quad (3a)$$

$$I_i(\nu) = \sum_j I_j L_j(\nu - \nu_{0j}) \quad (3b)$$

where j is the number of a band, Γ_j – is the half width at the half maximum, ν_{0j} – is the origin of the band, I_j – is IR intensity A_j (km/mol) or Raman activity S_j (Å^4/amu). Then, taking into account all the conformers the whole spectrum can be obtained as:

$$I(\nu) = \sum_i P_i \cdot I_i(\nu) \quad (4)$$

Because of very small barrier between conformers 1 and 2 ($\sim$ 10 cm^{-1}, see Fig. 7), it is reasonable to simplify the consideration. As a rough approximation, we use the mean weighted spectrum of these forms, including their populations. Together with experimental frequencies, the results of such evaluations are given in Tables 4–7. The final spectra are reproduced on bottom panels of Figs. 1–4. They are obtained with the following values of width (Γ):

5 cm^{-1} for CH stretch, 2 cm^{-1} for other bands at T = 120 K, and 10 cm^{-1} for CH stretch, 5 cm^{-1} for other bands at T = 295 K. So that, the widths of particular bands in the simulated IR and Raman spectra and the widths of respective bands in the experimental spectra are comparable. Temperature measurements performed in liquid Kr at $T \sim$ 120–160 K did not reveal qualitative changes in IR spectrum of enflurane, except for quite observable broadening of all the bands registered.

Assignment of experimental bands has been performed with the help of comparison the measured and calculated spectra. The vibrational bands are numbered, as commonly accepted from high frequency CH stretch to low frequency ones (see Figs. 1–4). It should be recognized that the majority of the bands which belong to different conformers are strongly overlapped. However, there are few regions, where the bands ascribed to conformers *a*, *b*, *c* can be resolved. These are: ν_{13}, ν_{15} (Fig. 1), ν_{15}, ν_{16} (Fig. 3) for enflurane HH, and ν_{14} (Fig. 2), ν_{14}, ν_{16} (Fig. 4) for enflurane HD.

Finally, probe experiments performed for two component solutions of enflurane and acetone in liquid Kr have confirmed the possible participation of atoms H of both CHFCl and CHF_2 groups in hydrogen bond formation recently suggested [17]. The characteristic example is presented in Fig. 8. Complex formation results in the

Table 1
MP2/6-311++G(df,pd) predicted geometric parameters of the most stable conformers of enflurane.

	a_1	a_2	b_1	b_2	c_1	c_2
χ_1 ($Cl_2—C_1—C_5—O_8$), deg	−62.25	−63.86	−178.08	−179.10	−298.72	−299.69
χ_2, ($H_{10}—C_9—O_8—C_5$), deg	−16.47	17.54	−16.69	12.99	−19.85	17.89
χ_3, ($C_1—C_5—O_8—C_9$), deg	186.14	175.57	185.45	176.84	184.17	173.10
$r(C_1H_4)$, Å	1.0905	1.0906	1.0906	1.0906	1.0913	1.0914
$r(C_1Cl_2)$, Å	1.7460	1.7457	1.7483	1.7483	1.7461	1.7462
$r(C_1F_3)$, Å	1.3482	1.3484	1.3458	1.3459	1.3464	1.3461
$r(C_9H_{10})$, Å	1.0904	1.0906	1.0907	1.0904	1.0908	1.0908
$r(C_9F_{12})$, Å	1.3280	1.3288	1.3290	1.3283	1.3275	1.3281
$r(C_9F_{11})$ Å	1.3338	1.3325	1.3321	1.3337	1.3337	1.3328
ΔE_{el}, cm^{-1}	0	−6.6	93.8	106.6	39.1	45

Table 2
Calculated (MP2/6-311++G(df,pd)) harmonic (ω), anharmonic (ν) frequencies, IR intensities (A), Raman activities (S) and potential energy distribution (PED) for a_1 conformer of enflurane-HH.

N°	ω, cm^{-1}	ν, cm^{-1}	A, km/mol	S, Å^4/amu	PED
1	3172	3075	14	45	νC_9H_{10} (100)
2	3162	3045	5.4	64	νC_1H_4 (100)
3	1472	1436	39	2.4	$\beta H_{10}C_9O_8$ (83)
4	1427	1393	78	2.5	$\beta H_4C_1C_5$ (33), νC_1C_5 (26), $\beta H_{10}C_9O_8$ (10)
5	1413	1385	53	2.1	$\gamma H_{10}C_9O_8$ (87)
6	1349	1323	24	2.9	$\gamma H_4C_1C_5$ (82)
7	1327	1297	122	3.0	$\beta H_4C_1C_5$ (38), νC_5F_7 (22), νC_1C_5 (10)
8	1269	1238	234	1.1	νC_5O_8 (54), νC_5F_6 (11)
9	1226	1200	330	1.9	νC_9F_{12} (62), $\gamma F_{12}C_9O_8$ (10)
10	1188	1163	531	2.5	νC_9F_{11} (57), $\gamma F_{12}C_9O_8$ (10)
11	1183	1156	150	2.7	νC_1F_3 (29), νC_5F_6 (17), νC_9O_8 (11)
12	1168	1143	117	2.5	νC_1F_3 (43), $\nu_{as}C_5F_6F_7$ (28), $\beta H_4C_1C_5$ (10)
13	1100	1075	124	3.8	νC_9O_8 (58), νC_1F_3 (11)
14	932	914	63	1.5	$\nu_sC_5F_6F_7$ (34), νC_1Cl_2 (29), νC_1C_5 (11)
15	876	861	59	7.2	νC_1Cl_2 (30), νC_5F_7 (15), $\beta F_6C_5C_1$ (12)
16	797	786	53	2.4	$\beta C_1C_5F_7$, $\gamma F_3C_1C_5$ (13), $\beta F_3C_1C_5$ (12)
17	670	662	0.9	2.5	$\gamma F_{12}C_9O_8$ (17), $\beta F_7C_5O_8$ (16), $\beta O_8C_9F_{11}$ (13)
18	596	590	9.8	0.5	$\gamma F_{12}C_9O_8$ (30), $\beta F_7C_5O_8$ (22), $\beta O_8C_9F_{11}$ (19)
19	586	582	8.8	0.6	$\beta C_5F_6F_7$ (33), $\beta O_8C_9F_{12}$ (25), $\beta F_6C_5C_1$ (10)
20	507	499	4.5	2.0	$\beta F_7C_5O_8$ (16), $\beta O_8C_9F_{11}$ (13), $\beta C_1C_5O_8$ (12)
21	450	443	4.5	2.3	$\beta O_8C_9F_{12}$ (27), $\beta C_5F_6F_7$ (21), νC_1Cl_2 (17)
22	428	424	2.9	0.6	$\gamma F_3C_1C_5$ (33), $\beta O_8C_9F_{11}$ (24), $\beta F_7C_5O_8$ (12)
23	350	345	0.6	1.9	$\beta O_8C_9F_{12}$ (14), $\beta F_3C_1C_5$ (13), $\beta F_6C_5C_1$ (11)
24	314	309	1.7	1.0	$\beta F_3C_1C_5$ (39), $\beta F_6C_5C_1$ (23), νC_1C_5 (16)
25	261	257	1.3	0.4	$\beta C_1C_5F_7$ (43), $\beta C_5O_8C_9$ (25), $\gamma F_3C_1C_5$ (10)
26	211	205	3.0	0.4	$\beta C_5C_1Cl_2$ (46), $\beta C_5O_8C_9$ (22), $\beta C_1C_5F_7$ (10)
27	123	116	2.1	0.2	$\beta C_1C_5O_8$ (45), $\beta C_5O_8C_9$ (26), $\beta C_5C_1Cl_2$ (12)
28	79	76	0.07	0.2	$\tau O_8C_5C_1Cl_2$ (91)
29	59	52	0.6	0.1	$\tau C_1C_5O_8C_9$ (89)
30	30	20	1.9	0.05	$\tau C_5O_8C_9F_{11}$ (88)

Table 3
Calculated (MP2/6-311++G(df,pd)) harmonic (ω), anharmonic (ν) frequencies, IR intensities (A), Raman activities (S) and potential energy distribution (PED) for a_1 conformer of enflurane-HD.

N°	ω, cm^{-1}	ν, cm^{-1}	A, km/mol	S, Å^4/amu	PED
1	3172	3076	14	46	νC_9H_{10} (100)
2	2330	2266	6.0	31	νC_1D_4 (100)
3	1472	1436	44	2.6	$\beta H_{10}C_9O_8$ (83)
4	1413	1385	62	2.3	$\gamma H_{10}C_9O_8$ (85)
5	1393	1362	127	1.9	νC_1C_5 (38)
6	1277	1246	230	1.0	νC_5O_8 (48), $\nu_sC_5F_6F_7$ (16)
7	1231	1203	450	0.8	$\nu_{as}C_5F_6F_7$ (43), $\nu_{as}C_9F_{11}F_{12}$ (27), $\beta C_5O_8C_9$ (10)
8	1223	1199	20	4.9	νC_9F_{12} (48), νC_1F_3 (16), $\beta F_{12}C_9F_{11}$ (12)
9	1192	1165	382	1.8	νC_1F_3 (34), $\nu_{as}F_{12}C_9O_8$ (26), νC_5F_6 (12)
10	1185	1158	248	2.3	νC_9F_{11} (67)
11	1109	1082	209	3.5	νC_9O_8 (50), νC_1F_3 (15)
12	1048	1029	84	0.7	$\gamma D_4C_1Cl_2$ (40), νC_5F_6 (18), νC_1Cl_2 (12)
13	997	982	10	3.9	$\gamma D_4C_1C_5$ (53), $\beta F_3C_1C_5$ (18), νC_1F_3 (14)
14	878	864	35	2.0	$\nu_sC_5F_6F_7$ (34), $\beta C_1C_5F_6$ (11)
15	816	804	30	5.3	νC_1Cl_2 (46), γD4C1Cl$_2$ (39)
16	772	761	40	2.8	νC_5F_7 (14), νC_5C_1 (10), $\beta F_7C_5C_1$ (10)
17	666	6595	1.1	2.6	$\beta C_5O_8C_9$ (19), $\beta F_{12}C_9F_{11}$ (15), $\beta F_{11}C_9O_8$ (13)
18	595	588	9.8	0.5	$\beta F_{12}C_9F_{11}$ (33), $\beta C_5O_8C_9$ (19), $\beta F_{11}C_9O_8$ (18)
19	580	574	9.9	0.4	$\beta C_5F_6F_7$ (32), $\gamma O_8C_9F_{12}$ (23)
20	505	496	4.5	1.9	$\beta F_7C_5O_8$ (16), $\beta O_8C_9F_{11}$ (13), $\beta C_1C_5O_8$ (12)
21	447	440	4.2	2.3	$\beta O_8C_9F_{12}$ (27), $\beta C_5F_6F_7$ (21), νC_1Cl_2 (17)
22	427	422	3.0	0.7	$\gamma F_3C_1C_5$ (33), $\beta O_8C_9F_{11}$ (24), $\beta F_7C_5O_8$ (12)
23	349	344	0.6	1.8	$\beta O_8C_9F_{12}$ (14), $\beta F_3C_1C_5$ (13), $\beta F_6C_5C_1$ (11)
24	314	309	1.7	1.0	$\beta F_3C_1C_5$ (39), $\beta F_6C_5C_1$ (23), νC_1C_5 (16)
25	260	256	1.3	0.4	$\beta C_1C_5F_7$ (43), $\beta C_5O_8C_9$ (25), $\gamma F_3C_1C_5$ (10)
26	210	205	3.0	0.4	$\beta C_5C_1Cl_2$ (46), $\beta C_5O_8C_9$ (22), $\beta C_1C_5F_7$ (10)
27	123	114	2.1	0.2	$\beta C_1C_5O_8$ (45), $\beta C_5O_8C_9$ (26), $\beta C_5C_1Cl_2$ (12)
28	76	75	0.06	0.2	$\tau O_8C_5C_1Cl_2$ (91)
29	59	52	0.7	0.1	$\tau C_1C_5O_8C_9$ (89)
30	29	21	1.8	0.05	$\tau C_5O_8C_9F_{11}$ (88)

blue shift effect, which is stronger in the case of atom H of CHF_2 group. Namely $\Delta\nu_1^{c\text{-}m}\sim+22$ cm^{-1}, $\Delta\nu_2^{c\text{-}m}\sim+11$ cm^{-1} However the intensity of respective CH stretch band ν_2 is noticeably larger in the case of more ''acidic'' hydrogen of CHFCl group. The effect is compatible with the feature of the dipole moment function [18,19]. In the case of high frequency CH stretch ν_1 the dominative component of the first derivative of the dipole moment is directed along the CH bond and is negative. It is worth noting incomplete

Table 4
Measured frequencies ν (cm^{-1}); calculated (MP2/6-311++G(df,pd)) mean weighted frequencies $\langle\nu\rangle$ (cm^{-1}) and IR intensities $\langle A\rangle$ (km/mol) in the IR spectrum of enflurane HH at T = 120 K.

N	Calculation						Kr_{liq}, 120 K
	a		*b*		*c*		
	$\langle\nu\rangle$	$\langle A\rangle$	$\langle\nu\rangle$	$\langle A\rangle$	$\langle\nu\rangle$	$\langle A\rangle$	ν
1	3075	7.80	3075	1.77	3071	4.89	3023
2	3045	3.05	3044	0.67	3037	1.70	2996
3	1436	21.4	1437	5.08	1438	11.69	1408
4	1393	41.7	1396	9.40	1399	14.94	1373
5	1386	31.6	1387	7.59	1385	17.06	1362
6	1323	18.5	1323	6.15	1326	15.08	(1304•), 1297
7	1300	68.5	1300	12.1	1324	51.71	(1282*), 1270
8	1238	130	1227	25.2	1209	121	1207(*a*), 1192(*c*)
9	1195	187	1197	50.7	1189	79.7	1172, 1162,1152, 1130,1112, 1102,1098
10	1167	248	1182	25.3	1175	126	
11	1152	141	1158	55.4	1157	9.74	
12	1143	57	1144	10.1	1143	28.6	
13	1075	70.0	1090	30.7	1095	83.7	1068(*c*), 1063(*b*), 1045(*a*)
14	916	36.5	919	0.58	932	11.6	906(*c*), 886(*a*)
15	862	32.5	849	9.93	877	23.3	841(*c*), 831(*a*), 819(*b*)
16	787	30.2	772	8.25	717	6.72	–
17	656	0.97	664	0.12	660	2.82	–
18	595	4.70	594	1.00	612	0.99	–
19	581	4.79	576	1.70	560	5.98	–
20	493	3.40	501	0.34	498	2.67	–
21	446	2.57	467	1.24	459	3.76	–
22	424	1.20	414	0.20	441	0.61	–
23	340	0.45	362	0.22	357	0.17	–
24	311	0.91	270	0.06	320	0.20	–
25	259	0.71	243	0.11	239	1.45	–
26	207	1.76	237	0.65	198	0.41	–
27	118	1.14	113	0.15	119	0.06	–
28	78	0.08	80	0.04	81	0.14	–
29	51	0.40	55	0.11	49	0.31	–
30	23	0.95	27	0.16	28	0.17	–

Notes: •, * – see Fig. 1.

Table 5
Measured frequencies ν (cm^{-1}); calculated (MP2/6-311++G(df,pd)) mean weighted frequencies $\langle\nu\rangle$ (cm^{-1}) and IR intensities $\langle A\rangle$ (km/mol) in the IR spectrum of enflurane HD at T = 120 K.

N	Calculation						Kr_{liq}, 120 K
	a		*b*		*c*		
	$\langle\nu\rangle$	$\langle A\rangle$	$\langle\nu\rangle$	$\langle A\rangle$	$\langle\nu\rangle$	$\langle A\rangle$	ν
1	3075	7.83	3075	1.86	3072	4.60	3024
2	2267	3.39	2263	0.79	2254	1.92	–
3	1436	24.6	1435	6.21	1436	11.0	1407
4	1386	35.4	1387	8.06	1387	18.7	1363
5	1362	72.8	1364	18.4	1365	45.4	1340
6	1249	135	1242	28.5	1262	59.1	1216(*c*), 1204(*a*)
7	1205	208	1208	44.2	1202	111	1162
8	1182	85.6	1191	31.7	1179	127	1141
9	1168	156	1175	18.5	1162	20.2	1123
10	1157	170	1158	31.5	1154	41.1	1115
11	1082	115	1107	62.4	1102	88.7	1075(*b*,*c*), 1049(*a*)
12	1029	51.5	1016	2.66	1030	35.0	994
13	983	5.98	986	0.48	982	0.61	965
14	864	19.4	861	5.69	899	6.33	880(*c*), 844(*a*)
15	804	17.1	799	4.09	805	9.54	–
16	762	22.7	746	6.43	704	3.26	–
17	646	1.40	659	0.15	646	2.55	–
18	594	4.74	591	1.21	612	0.89	–
19	574	5.15	574	1.71	552	5.70	–
20	491	3.57	494	0.41	494	2.75	–
21	443	2.43	465	1.22	457	3.90	–
22	422	1.20	413	0.21	440	0.57	–
23	339	0.44	361	0.24	356	0.17	–
24	311	0.92	269	0.06	320	0.19	–
25	257	0.71	243	0.12	239	1.40	–
26	207	1.79	236	0.68	198	0.39	–
27	117	1.13	113	0.15	117	0.06	–
28	77	0.08	79	0.04	79	0.14	–
29	50	0.38	55	0.13	49	0.30	–
30	23	0.96	26	0.17	28	0.17	–

Table 6
Measured frequencies v (cm^{-1}); calculated (MP2/6-311++G(df,pd)) mean weighted frequencies $\langle v \rangle$ (cm^{-1}) and Raman activities $\langle S \rangle$ ($Å^4$/amu) in the Raman spectrum of enflurane HH at T = 295 K.

N	Calculation						Liquid, 295 K
	a		*b*		*c*		
	$\langle v \rangle$	$\langle S \rangle$	$\langle v \rangle$	$\langle S \rangle$	$\langle v \rangle$	$\langle S \rangle$	v
1	3075	25.9	3075	9.26	3071	16.2	3035
2	3045	36.4	3044	13.8	3037	24.9	3006
3	1436	1.45	1437	0.62	1438	0.87	1406
4	1393	1.37	1396	0.57	1399	0.86	1368
5	1386	1.22	1387	0.45	1385	0.80	
6	1323	1.65	1323	0.48	1325	0.84	1298
7	1300	1.64	1300	0.82	1323	1.02	1271
8	1238	0.65	1227	0.24	1208	0.41	1200
9	1195	1.21	1197	0.45	1188	0.63	1140
10	1167	1.34	1172	0.54	1176	0.82	1100
11	1154	1.40	1157	0.34	1157	0.84	1070
12	1143	1.54	1144	0.47	1143	0.70	
13	1075	2.13	1090	1.39	1095	1.17	
14	916	0.84	919	0.36	932	0.33	904(*c*), 888(*a*, *b*)
15	862	4.12	849	1.97	877	2.50	838(*c*), 829(*a*), 819(*b*)
16	787	1.36	772	0.35	717	0.31	768(*a*), 754(*b*), 708(*c*)
17	660	1.14	666	0.43	660	1.71	645
18	600	0.48	602	0.15	614	0.51	600(*c*) 571(*a*, *b*)
19	581	0.40	576	0.10	560	0.25	555
20	498	0.77	497	0.42	497	0.26	490
21	447	1.53	464	0.25	459	0.42	432
22	423	0.44	414	0.21	441	0.63	403
23	341	1.05	363	0.44	356	0.57	356(*c*), 339(*a*)
24	312	0.60	270	0.30	320	0.32	316(*c*), 310(*a*), 269(*b*)
25	258	0.18	243	0.15	239	0.18	244
26	206	0.20	237	0.05	198	0.09	211
27	119	0.10	114	0.02	119	0.06	–
28	77	0.10	80	0.03	81	0.07	–
29	51	0.07	55	0.00	49	0.06	–
30	25	0.04	28	0.02	27	0.02	–

Table 7
Measured frequencies v (cm^{-1}); calculated (MP2/6-311++G(df,pd)) mean weighted frequencies $\langle v \rangle$ (cm^{-1}) and Raman activities $\langle S \rangle$ ($Å^4$/amu) in the Raman spectrum of enflurane HD at T = 295 K.

N	Calculation						Liquid, 295 K
	a		*b*		*c*		
	$\langle v \rangle$	$\langle S \rangle$	$\langle v \rangle$	$\langle S \rangle$	$\langle v \rangle$	$\langle S \rangle$	v
1	3075	21.0	3075	9.70	3072	15.3	3038
2	2267	14.1	2263	6.75	2254	12.1	2245
3	1436	1.18	1435	0.63	1436	0.87	1406
4	1386	1.00	1387	0.48	1387	0.68	1367
5	1362	0.95	1364	0.50	1365	0.78	1337
6	1249	0.41	1242	0.33	1262	0.50	
7	1205	0.69	1207	0.13	1201	0.48	1164
8	1182	1.74	1193	0.72	1179	0.65	1117
9	1168	1.01	1171	0.50	1162	0.74	1080
10	1157	0.99	1157	0.38	1154	0.65	
11	1082	1.56	1107	1.46	1102	1.22	
12	1029	0.32	1016	0.23	1030	0.26	
13	983	1.78	986	0.84	982	1.23	969
14	864	0.93	861	0.39	899	0.59	880(*c*), 844(*a*)
15	804	2.41	799	1.67	805	1.77	771
16	762	1.26	747	0.42	704	0.47	746(*a*), 729(*b*), 694(*c*)
17	646	0.97	665	0.44	646	1.31	630
18	594	0.38	598	0.14	613	0.51	563
19	574	0.26	573	0.09	552	0.30	543
20	491	0.56	494	0.34	492	0.26	486
21	443	1.25	464	0.35	458	0.41	427
22	422	0.37	413	0.21	440	0.63	405
23	339	0.84	362	0.45	355	0.55	358(*b*, *c*), 338(*a*)
24	311	0.48	269	0.32	320	0.31	268(*b*), 313(*a*, *c*)
25	257	0.15	243	0.15	239	0.17	244
26	207	0.15	236	0.04	198	0.09	209
27	117	0.08	113	0.02	118	0.06	–
28	77	0.08	79	0.03	79	0.06	–
29	50	0.06	55	0.00	49	0.06	–
30	23	0.03	26	0.03	28	0.02	–

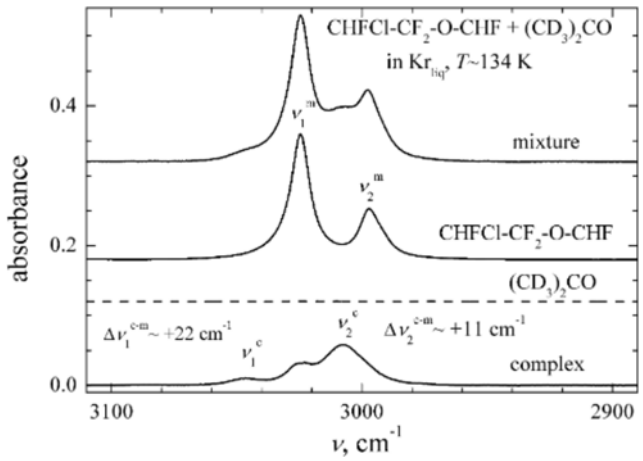

Fig. 8. Region of CH stretch bands ν_1, ν_2. Enflurane ($\sim 6 \cdot 10^{17}$molecules/cm^3) + $(CD_3)_2CO$ ($\sim 4 \cdot 10^{17}$molecules/cm^3) in liquid Kr at $T \sim 134$ K.

cancellation of ν_1^m band after subtraction procedure (bottom band on Fig. 8). This is due to slight change of the frequency of this band in the case of interaction of acetone with more "acidic" atom H of CHFCl group. Ab initio calculations confirm this experimental result.

5. Conclusions

The IR spectrum of diluted solutions (10^{17}–10^{18} molecules/cm^3) of enflurane HH (CHFCl—CF_2—O—CHF_2) and enflurane HD (CDFCl—CF_2—O—CHF_2) in liquefied Kr is obtained and analyzed in the range c.a. 800–4000 cm^{-1}. Additionally the Raman spectrum of liquid enflurane is measured at room temperature.

The ab initio calculations, performed at MP2/6-311++G(df,pd) level predict 6 most stable conformers of enflurane. They differ by two dihedral angles: χ_1 (Cl_2—C_1—C_5—O_8) and χ_2 (H_{10}—C_9—O_8—C_5). The barrier between pairs of conformers, differing by dihedral angle χ_2 is very small (≤ 10 cm^{-1}). This result suggests that only three conformers might be experimentally detected, as it was done in the work on gas electron diffraction studies [15].

The vibrational frequencies are calculated at the same level using "anharm" option in Gaussian. Infrared intensity and Raman scattering activity are also obtained for all the conformers found. PED is calculated for the most stable conformer of enflurane. The results obtained for normal vibrations of enflurane HH are similar to the data obtained earlier at noticeably lower level of theory [16]. The exception concerns the ν_4 and ν_5 vibrations for which the serious disagreement has been revealed.

The majority of vibrational bands of different conformers are strongly overlapped. However, there are few characteristic regions in IR and Raman spectra of H/D substituted enflurane, where the bands ascribed to three conformers can be resolved.

Both atoms H of CHFCl and CHF_2 groups of enflurane can participate in H bond formation characterized by blue shifting effect in the case of interactions with acetone.

Conflict of interest

There is no conflict of interest.

Acknowledgements

The work was supported by the Russian Foundation for Basic Research N° 14-03-00716, National Science Centre for research funding N° 2012/05/B/ST4/02029 and Saint-Petersburg State University – Russia (Grant 11.38.265.2014). W.H. acknowledges the Flemish Fund for Scientific Research (FWO Vlaanderen) and BOF funding agency of Antwerp University for support. The calculations have been performed using the computer resources of the Resource Center of Saint-Petersburg State University (http://cc.spbu.ru), of the Wrocław Center for Networking and Supercomputing (http://www.wcss.wroc.pl), and partly of the Flemish Supercomputer Center. The spectroscopic measurements were partly performed on the apparatus of the Resource Center Geomodel of Saint-Petersburg State University – Russia.

Appendix A. Supplementary data

Supplementary data associated with this article can be found, in the online version, at http://dx.doi.org/10.1016/j.chemphys.2015.03.010.

References

[1] B.J. van der Veken, W.A. Herrebout, R. Szostak, D.N. Shchepkin, Z. Havlas, P. Hobza, J. Am. Chem. Soc. 123 (2001) 12290.
[2] Y. Gu, T. Kar, S. Scheiner, J. Am. Chem. Soc. 121 (1999) 9411.
[3] W. Qian, S. Krimm, J. Phys. Chem. A 106 (2002) 11663.
[4] K. Hermansson, J. Phys. Chem. A 106 (2002) 4695.
[5] S.M. Melikova, K.S. Rutkowski, P. Rodziewicz, A. Koll, Chem. Phys. Lett. 352 (2002) 301.
[6] A. Karpfen, E.S. Kryachko, J. Phys. Chem. A 107 (2003) 9724.
[7] E.S. Kryachko, A. Karpfen, Chem. Phys. 329 (2006) 313.
[8] S. Scheiner, T. Kar, J. Phys. Chem. A 112 (2008) (1860) 11854.
[9] S.A. McDowell, Chem. Phys. Lett. 424 (2006) 239.
[10] P. Rodziewicz, K.S. Rutkowski, S.M. Melikova, A. Koll, Chem. Phys. Chem 6 (2005) 1282.
[11] K.S. Rutkowski, S.M. Melikova, P. Rodziewicz, W.A. Herrebout, B.J. Van der Veken, A. Koll, J. Mol. Struct. 880 (2008) 64.
[12] B. Czarnik-Matusewicz, D. Michalska, C. Sandorfy, Th. Zeegers-Huyskens, Chem. Phys. 322 (2006) 331.
[13] B. Michelsen, W.A. Herrebout, B.J. van der Veken, Chem. Phys. Chem. 9 (2008) 1693.
[14] B. Michelsen, J.J.J. Dom, B.J. van der Veken, S. Hesse, Z. Xue, M.A. Suhm, W.A. Herrebout, Phys. Chem. Chem. Phys. 12 (2010) 14034.
[15] A. Pfeiffer, H.G. Mack, H. Oberhammer, J. Am. Chem. Soc. 120 (1998) 6384.
[16] D. Michalska, D.C. Bienko, B. Czarnik-Matusewicz, M. Wierzejewska, C. Sandorfy, Th. Zeegers-Huyskens, J. Phys. Chem. B 111 (2007) 12228.
[17] W. Zierkiewicz, B. Czarnik-Matusewicz, D. Michalska, J. Phys. Chem. A 115 (2011) 11362.
[18] W. Zierkiewicz, R. Zalesny, P. Hobza, Phys. Chem. Chem. Phys. 15 (2013) 6001.
[19] S.M. Melikova, K.S. Rutkowski, B. Czarnik-Matusewicz, M. Rospenk, Chem. Phys. Lett. 604 (2014) 68.
[20] T.R. Burke Jr., L.R. Pohl, J. Labelled Compd. Radiopharm. 18 (1981) 663.
[21] M.J. Frisch, G.W. Trucks, H.B. Schlegel, G.E. Scuseria, M.A. Robb, J.R. Cheeseman, G.Scalmani, V. Barone, B. Mennucci, G.A. Petersson, H. Nakatsuji, M. Caricato, X. Li, H.P. Hratchian, A.F. Izmaylov, J. Bloino, G. Zheng, J.L. Sonnenberg, M. Hada, M. Ehara, K. Toyota, R. Fukuda, J. Hasegawa, M. Ishida, T. Nakajima, Y. Honda, O. Kitao, H. Nakai, T. Vreven, J.A. Montgomery, Jr., J.E. Peralta, F. Ogliaro, M. Bearpark, J.J. Heyd, E. Brothers, K.N. Kudin, V.N. Staroverov, T. Keith, R. Kobayashi, J. Normand, K. Raghavachari, A. Rendell, J.C. Burant, S.S. Iyengar, J. Tomasi, M. Cossi, N. Rega, J.M. Millam, M. Klene, J.E. Knox, J.B. Cross, V. Bakken, C. Adamo, J. Jaramillo, R. Gomperts, R.E. Stratmann, O. Yazyev, A.J. Austin, R. Cammi, C. Pomelli, J.W. Ochterski, R.L. Martin, K. Morokuma, V.G. Zakrzewski, G.A. Voth, P. Salvador, J.J. Dannenberg, S. Dapprich, A.D. Daniels, O. Farkas, J.B. Foresman, J.V. Ortiz, J. Cioslowski, D.J. Fox, Gaussian 09, Revision C.01. Gaussian Inc, Wallingford CT, 2010.
[22] C. Møller, M.S. Plesset, Phys. Rev. 46 (1934) 618.
[23] M.H. Jamróz, Spectrochim. Acta 114 (2013) 220.
[24] M.J. Nowak, L. Lopinski, D.C. Bienko, D. Michalska, Spectrochim. Acta A53 (1997) 855.
[25] A.V. Cherevatova, T.D. Kolomiitsova, D.N. Shchepkin, K.G. Tokhadze, Z. Mielke, S. Coussan, P. Roubin, J. Mol. Spectrosc. 238 (2006) 64.
[26] G. Placzek. Rayleigh Streuung und Raman – Effekt/Handbuch der Radiologie/ Ed. by E. Marx. – Leipzig: Academische Verlagsgesellschaft M.B.H., 1934. – Bd.6, T.2. – pp. 205–374.
[27] D. Michalska, R. Wysokinski, Chem. Phys. Lett. 403 (2005) 211.
[28] V.A. Kondaurov, S.M. Melikova, D.N. Shchepkin, Opt. Spectrosc. 56 (1984) 1020.
[29] K.S Rutkowski, S.M. Melikova, D.N. Shchepkin, Vibr. Spectrosc. 24 (2000) 277.